Progress In Electromagnetics Research M, Vol. 41, 85–93, 2015

Incomplete Bessel Polynomials: A New Class of Special Polynomials for Electromagnetics

Diego Caratelli[1, 2, *], Galina Babur[3], Alexander Shibelgut[3], and Oleg Stukach[2]

Abstract—A new class of incomplete Bessel polynomials is introduced, and its application to the solution of electromagnetic problems regarding transient wave radiation phenomena in truncated spherical structures is discussed. The general definition and main analytical properties of said special functions are provided. The definition is such that the interrelationships between the incomplete polynomials parallel, as far as it is feasible, those for canonical Bessel polynomials.

1. INTRODUCTION

Special functions are used to express exact or approximate analytical solutions of complex physical problems [1]. They are widely adopted in various scientific fields, such as mathematical physics and electromagnetics. Recently, incomplete Hankel functions have been introduced in [2] to determine the electromagnetic field distribution associated with progressive and evanescent wave contributions excited in truncated cylindrical structures. On the other hand, as shown in [3], the transient electromagnetic field radiated in Fraunhofer region by a general antenna can be expressed as a non-uniform spherical wave expansion in terms of incomplete modified spherical Bessel functions (*IMSBFs*) [4].

In this paper, a new class of incomplete Bessel polynomials (*IBPs*) is introduced in order to allow for the analytical closed-form evaluation of *IMSBFs* of arbitrary integral order n. The analytical properties of the considered class of functions, with particular attention to the relevant governing differential equation and recurrence formulae, are derived and discussed thoroughly. Furthermore, the general theory is validated by application to the electromagnetic characterization of a dielectric lens antenna and comparison with a brute-force numerical procedure.

2. DEFINITION

Let us consider an antenna operating in free-space, enclosed by a Huygens spherical surface S_h having radius R_h (see Fig. 1). By using the approach based on the singularity expansion method (*SEM*) detailed in [3], the space-time distribution of the electromagnetic field radiated by the structure under analysis is found to be:

$$\mathcal{E}(\mathbf{r},\tau) = \frac{1}{4\pi r c_0}\sum_{n=0}^{N}\sum_{m=-n}^{n}\sum_{k=1}^{K}\psi_n\left(s_{n,m,k}t_h,\frac{\tau}{t_h}\right)Y_n^m(\vartheta,\varphi)\,\mathbf{e}_{n,m,k}, \tag{1}$$

$$\mathcal{H}(\mathbf{r},\tau) = \frac{1}{\eta_0}\hat{\mathbf{r}}\times\mathcal{E}(\mathbf{r},\tau), \tag{2}$$

Received 31 December 2014, Accepted 13 February 2015, Scheduled 19 February 2015

* Corresponding author: Diego Caratelli (diego.caratelli@antennacompany.com).
[1] The Antenna Company Nederland B.V., Grebbeweg 111, 3911AV Rhenen, the Netherlands. [2] Tomsk Polytechnic University, 84/3 Sovetskaya Street, 634050 Tomsk, Russia. [3] Tomsk State University of Control Systems and Radio Electronics, 40 Lenina Prospect, 634050 Tomsk, Russia.

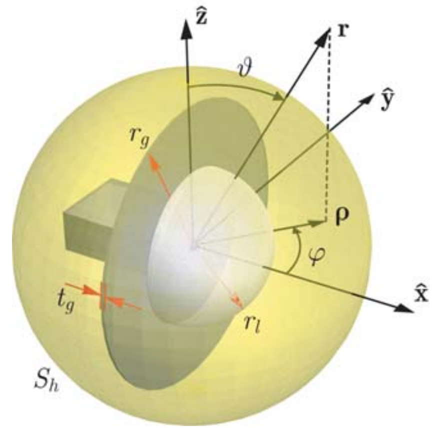

Figure 1. Dielectric lens antenna enclosed by a spherical Huygens surface S_h. The coordinate system adopted to express the electromagnetic field quantities is also shown.

where $Y_n^m(\vartheta,\varphi)$ denotes the spherical harmonic of orders n and m [5], and:

$$\psi_n(\xi,w) = \xi e^{\xi w} i_n(\xi, \min\{1,w\})\, u(1+w), \tag{3}$$

with $i_n(\cdot,\cdot)$ being the *IMSBF* of order n and $u(\cdot)$ the usual Heaviside distribution [6]. In equations (1) and (2), c_0 and η_0 denote the speed of light and the free-space wave impedance respectively, $t_h = R_h/c_0$ is the propagation time from the center to the surface of the Huygens sphere S_h enclosing the antenna under test, and $\tau = t - r/c_0$ is the spherical-wave delayed time. As it can be easily inferred, the considered electromagnetic field expansion consists in the superposition of non-uniform spherical waves propagating with complex frequencies $s_{n,m,k}$ and residual polarization vectors $\mathbf{e}_{n,m,k}$ depending on the damped natural resonant processes occurring in the structure, whose characterization is carried out by means of the pole/residue fitting procedure detailed in [3].

According to the definition in [4], the following integral representation in Whittaker's form [7] holds true:

$$i_n(\xi,w) = \frac{1}{2}\int_{-w}^{1} e^{\xi z} P_n(z)\, dz, \tag{4}$$

where $P_n(\cdot)$ is the Legendre polynomial of degree n featuring the explicit expression [6]:

$$P_n(z) = \sum_{k=0}^{n} \binom{n}{k}\binom{-n-1}{k}\left(\frac{1-z}{2}\right)^k. \tag{5}$$

It is straightforward to show, from combining (5) with (4), that:

$$i_n(\xi,w) = i_n(\xi) - e^{\xi}\sum_{k=0}^{n}\binom{n}{k}\binom{-n-1}{k}\frac{\Gamma(k+1,(1+w)\,\xi) - \Gamma(k+1,2\xi)}{(2\xi)^{k+1}}, \tag{6}$$

with $\Gamma(a,z) = \int_z^{+\infty} t^{a-1}e^{-t}dt$ and $i_n(z) = i_n(z,1) = \sqrt{\frac{1}{2}\pi/z}\, I_{n+1/2}(z)$ denoting the incomplete Gamma function, and the canonical modified spherical Bessel function of the first kind and order n, respectively. Upon noticing that:

$$\binom{-n-1}{k} = (-1)^k \frac{(n+k)!}{k!\,n!}, \tag{7}$$

and making use of the following integral expression of the modified spherical Bessel function of the second kind and order $n > -1/2$:

$$K_n(z) = \sqrt{\frac{\pi}{2z}}\frac{e^{-z}}{\left(n-\frac{1}{2}\right)!}\int_0^{+\infty} e^{-t}\left(t - \frac{t^2}{2z}\right)^{n-\frac{1}{2}} dt = \sqrt{\pi}e^{-z}\sum_{k=0}^{+\infty}\frac{\left(n+k-\frac{1}{2}\right)!}{k!\left(n-k-\frac{1}{2}\right)!}(2z)^{-k-\frac{1}{2}}, \tag{8}$$

it may be easily verified that:

$$\sum_{k=0}^{n}\binom{n}{k}\binom{-n-1}{k}\frac{\Gamma\left(k+1,2\xi\right)}{\left(2\xi\right)^{k+1}}=-e^{-\xi}\left[i_n\left(\xi\right)-\frac{1}{\pi}k_n\left(-\xi\right)\right], \tag{9}$$

where $k_n\left(z\right)=\sqrt{\frac{1}{2}\pi/z}\,K_{n+1/2}\left(z\right)$ is the modified spherical Bessel function of the second kind and order n [8]. Furthermore, by virtue of the identity:

$$\Gamma\left(k+1,z\right)=k!\,e^{-z}\sum_{m=0}^{k}\frac{z^m}{m!}, \tag{10}$$

holding for integer values of the parameter k, one can derive, after some mathematical manipulations:

$$\sum_{k=0}^{n}\binom{n}{k}\binom{-n-1}{k}\frac{\Gamma\left(k+1,\left(1+w\right)\xi\right)}{\left(2\xi\right)^{k+1}}=\frac{e^{-\left(1+w\right)\xi}}{2\xi}\sum_{k=0}^{n}y_{n,k}\left(-\frac{1}{\xi}\right)\frac{\left[\xi\left(1+w\right)\right]^k}{k!}, \tag{11}$$

this explicit expansion being expressed in terms of *IBPs* defined by the series:

$$y_{n,k}\left(z\right)=\sum_{m=k}^{n}\frac{\left(n+m\right)!}{m!\left(n-m\right)!}\left(\frac{z}{2}\right)^m, \tag{12}$$

From Equation (12), it can be easily seen that $y_{n,k}(z)$ coincides, for $k=0$, with the canonical Bessel polynomial (*BP*) of order n [9, 10]:

$$y_{n,0}\left(z\right)=y_n\left(z\right)=\frac{2}{\pi z}e^{1/z}k_n\left(\frac{1}{z}\right), \tag{13}$$

explaining why the terminology of calling $y_{n,k}(z)$ an incomplete polynomial is pertinent. Actually, there is a strong interrelationship between these sequences of special polynomials, the analytical properties of the former paralleling and generalizing those of the latter.

Finally, combining Equations (6), (9), and (11) yields the following closed-form analytical expression of the *IMSBF* of order n:

$$i_n\left(\xi,w\right)=\frac{1}{2\xi}\left\{e^{\xi}y_n\left(-\frac{1}{\xi}\right)-e^{-w\xi}\sum_{k=0}^{n}y_{n,k}\left(-\frac{1}{\xi}\right)\frac{\left[\xi\left(1+w\right)\right]^k}{k!}\right\}. \tag{14}$$

The typical distribution of an *IMSBF*, as evaluated by (14), is shown in Fig. 2. It is worth noting that, in the electromagnetic field theory regarding radiation and scattering from truncated structures, the right-hand side of (14) may be regarded as the superposition of a uniform wave contribution and different

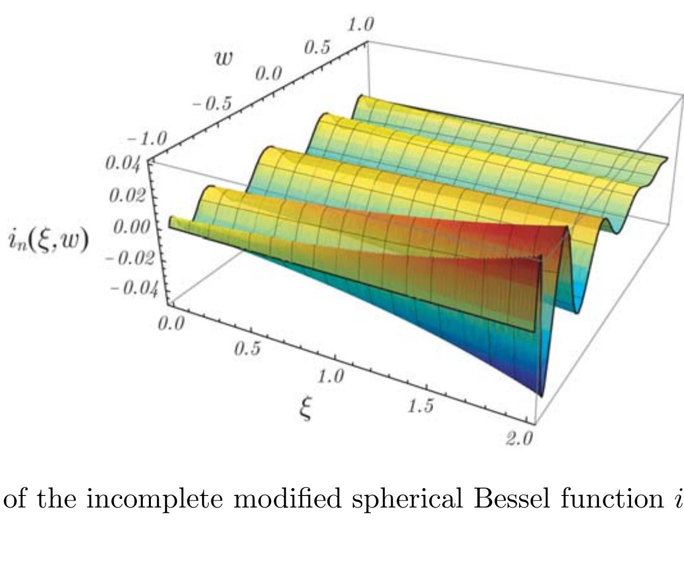

Figure 2. Distribution of the incomplete modified spherical Bessel function $i_n(\xi,w)$ of order $n=10$.

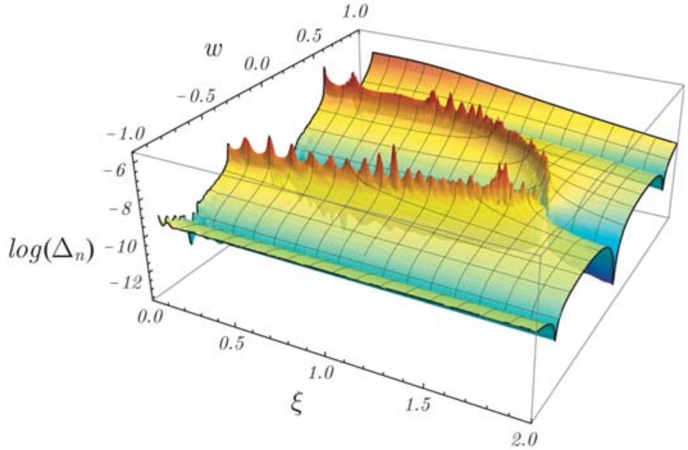

Figure 3. Relative deviation between the distributions of the incomplete modified spherical Bessel function $i_n(\xi, w)$ of order $n = 3$ as computed by numerical integration of the Whittaker's representation, and by means of the relevant *IBP* expansion.

higher-order terms, depending on the parameter w, related to the edge diffraction process occurring at the truncation of the sub-domain $\Omega_h(\vartheta, \varphi, \tau) = \{(\vartheta', \varphi') : \sin\vartheta \sin\vartheta' \cos(\varphi - \varphi') + \cos\vartheta \cos\vartheta' > -\tau/t_h\}$ of the Huygens sphere S_h that actually contributes to the radiated electromagnetic field value excited along the general angular direction (ϑ, φ) at a given delayed time τ.

The soundness of the theoretical findings reported in this section has been assessed numerically by evaluating the relative deviation Δ_n between the distributions of the *IMSBF* of general order n as computed by brute-force integration of the Whittaker's representation (4), and by using the *IBP* expansion (14), respectively. In this way, it has been observed that Δ_n is almost everywhere practically negligible (see Fig. 3) proving the correctness of the derived formulas. It is apparent, furthermore, that the *IBP* expansion is not only accurate but provides, also, a clear benefit in terms of computational efficiency, defined as the ratio of the time required for the calculation of the *IMSBFs* by means of the numerical integration of (4) and that using the closed-form expression (14). As a matter of fact, it has been numerically found out that the latter allows for a reduction of the computational burden by at least one order of magnitude.

3. ANALYTICAL PROPERTIES

In the previous section, the *IBPs* have been introduced and derived as the polynomial factors of the incomplete modified spherical Bessel functions $i_n(\cdot,\cdot)$ of integral order n. We now turn to the consideration of the analytical properties of this important class of special polynomials (see Fig. 4).

Upon setting for shortness:

$$\gamma_{n,m} = \frac{(n+m)!}{2^m m!\,(n-m)!} = \frac{(-1)^n}{2^m} \lim_{\mu\to m} \frac{\Gamma(-\mu)}{\Gamma(-\mu-n)\,\Gamma(-\mu+n+1)}, \tag{15}$$

the series representation of the general *IBP* can be written in a concise way as $y_{n,k}(z) = \sum_{m=k}^{n} \gamma_{n,m} z^m$, this expression being valid for every positive or negative integral order $m \in \mathbb{Z}$. In order to derive the differential equation defining $y_{n,k}(\cdot)$, let us first introduce the conventional Bessel operator [9, 10]:

$${}_y\mathcal{D}_{z,n} = z^2 \frac{d^2}{dz^2} + 2(z+1)\frac{d}{dz} - n(n+1), \tag{16}$$

such that ${}_y\mathcal{D}_{z,n}\, y_n(z) = 0$. By virtue of the identity:

$$\frac{d^p}{dz^p} y_{n,k}(z) = \frac{d^p}{dz^p} y_n(z) - \begin{cases} \displaystyle\sum_{m=p}^{k-1} \frac{m!}{(m-p)!} \gamma_{n,m} z^{m-p}, & 0 \leqslant p < k, \\ 0, & 0 \leqslant k \leqslant p, \end{cases} \tag{17}$$

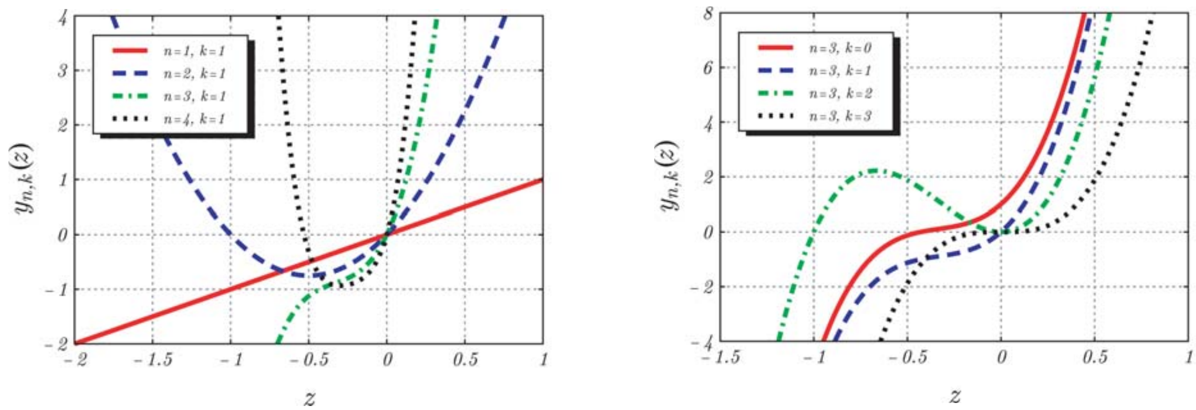

(a) (b)

Figure 4. Distribution of the incomplete Bessel polynomial $y_{n,k}(z)$ for different orders n (a) and k (b).

it is straightforward to show, after some algebra, that:

$$_{y}\mathcal{D}_{z,n}\, y_{n,k}\left(z\right) = 2k\gamma_{n,k} z^{k-1}, \tag{18}$$

for every $k \in \mathbb{Z}$. In a similar way, by using the explicit expansion (12), one may easily verify that the *IBPs* satisfy the following recurrence equations:

$$y_{n+1,k}\left(z\right) - \left(2n+1\right) z\, y_{n,k}\left(z\right) - y_{n-1,k}\left(z\right) = \left(2n+1\right)\gamma_{n,k-1} z^{k}, \tag{19}$$

$$z^2 y'_{n,k}\left(z\right) - \left(nz-1\right) y_{n,k}\left(z\right) - y_{n-1,k}\left(z\right) = \left(n-k+1\right)\gamma_{n,k-1} z^{k}, \tag{20}$$

$$z\left[y'_{n,k}\left(z\right) + y'_{n-1,k}\left(z\right)\right] - n\left[y_{n,k}\left(z\right) - y_{n-1,k}\left(z\right)\right] = 0, \tag{21}$$

$$z^2 y'_{n-1,k}\left(z\right) - y_{n,k}\left(z\right) + \left(nz+1\right) y_{n-1,k}\left(z\right) = -\left(n-k+1\right)\gamma_{n,k-1} z^{k}, \tag{22}$$

$$\left(nz+1\right) y'_{n,k}\left(z\right) + y'_{n-1,k}\left(z\right) - n^2 y_{n,k}\left(z\right) = n\left(n-k+1\right)\gamma_{n,k-1} z^{k-1}, \tag{23}$$

where the superscript $'$ denotes differentiation with respect to the variable z. It is not difficult to find out that formulas (19)–(23) degenerate into the well-known recurrence equations for canonical *BPs* as the index k is set to zero [9].

Starting from the expansion (12), the incomplete reverse Bessel polynomials (*IRBPs*) can be defined as the class of functions (see Fig. 5):

$$\theta_{n,k}\left(z\right) = z^n y_{n,k}\left(\frac{1}{z}\right) = \sum_{m=0}^{n-k} \frac{\left(2n-m\right)!}{m!\left(n-m\right)!}\frac{z^m}{2^{n-m}}. \tag{24}$$

featuring governing the differential equation:

$$_{\theta}\mathcal{D}_{z,n}\,\theta_{n,k}\left(z\right) = z\theta''_{n,k}\left(z\right) - 2\left(z+n\right)\theta'_{n,k}\left(z\right) + 2n\theta_{n,k}\left(z\right) = 2k\gamma_{n,k} z^{n-k}. \tag{25}$$

Clearly, $\theta_{n,k}\left(\cdot\right)$ generalize the canonical reverse *BP* of order n introduced in [10] as:

$$\theta_{n,0}\left(z\right) = \theta_n\left(z\right) = z^n y_n\left(\frac{1}{z}\right) = \frac{2}{\pi} z^{n+1} e^{z} k_n\left(z\right), \tag{26}$$

such that $_{\theta}\mathcal{D}_{z,n}\,\theta_n\left(z\right) = 0$. The definition (24) can find direct application in circuit theory, and synthesis of complex filter networks [11]. Here it is worth noting that, by trivial manipulation of (14), the general *IMSBF* can be expressed in terms of *IRBPs* as:

$$i_n\left(\xi, w\right) = \frac{\left(-1\right)^n}{2\xi^{n+1}}\left[e^{\xi}\theta_n\left(-\xi\right) - e^{-w\xi}\sum_{k=0}^{n}\frac{\xi^k\theta_{n,k}\left(-\xi\right)}{k!}\left(1+w\right)^k\right]. \tag{27}$$

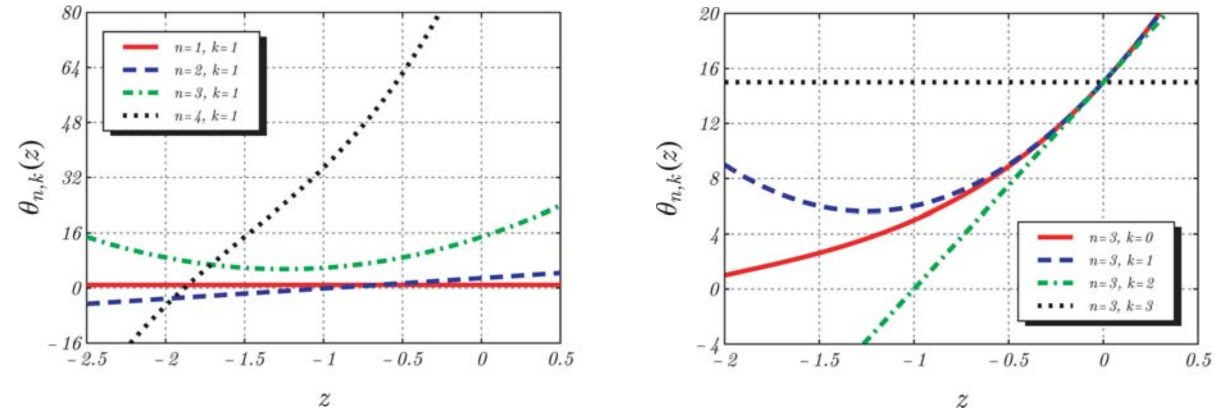

(a) (b)

Figure 5. Distribution of the incomplete reverse Bessel polynomial $\theta_{n,k}(z)$ for different orders n (a) and k (b).

4. NUMERICAL APPLICATION

The general theory detailed in the previous sections has been validated by application to the electromagnetic characterization of the hemispherical dielectric lens antenna sketched in Fig. 1. The considered lens features radius $r_l = 2.75\,\text{cm}$, and is assumed to be made out of polyvinylchloride (PVC) with relative permittivity $\varepsilon_r = 2.7$ and electrical loss tangent $\tan\delta = 0.003$. In order to reduce the back-radiation level, the radiating structure is integrated with a circular ground plane having radius $r_g = 5.0\,\text{cm}$ and thickness $t_g = 1.5\,\text{mm}$. Furthermore, as it appears from Fig. 1, the antenna is fed by means of a *WR90* rectangular waveguide with dimensions $a = 2.286\,\text{cm}$ and $b = 1.016\,\text{cm}$ filled up with the same dielectric material forming the lens.

The near-field full-wave analysis of the device has been performed by means of a locally conformal finite-difference time-domain ($FDTD$) scheme introduced in [12] for the accurate modeling of complex metal-dielectric electromagnetic structures avoiding the staircase approximation and the use of unstructured and/or stretched space lattices potentially suffering from significant numerical dispersion and instability [13]. In particular, the antenna has been meshed on a uniaxial perfectly matched layer backed uniform grid with spatial increment $\Delta h = 0.75\,\text{mm}$, where the excitation is carried out by means of the sinusoidally modulated Gaussian pulse with central frequency $f_0 = 7.0\,\text{GHz}$ and bandwidth $B = 2.0\,\text{GHz}$ defined by the expression:

$$\Pi_g(t) = \exp\left[-\left(\frac{t-T_0}{T_g}\right)^2\right]\sin(2\pi f_0 t)\,u(t)\,. \tag{28}$$

where the parameters $T_g = \frac{2}{\pi}\sqrt{\ln 10}/B \simeq 0.483\,\text{ns}$ and $T_0 = 4T_g$ have been selected in order to give the source signal significant energy in the range between the cut-off frequencies at $-10\,\text{dB}$ level, namely $f_{\min} = f_0 - B/2 = 6.0\,\text{GHz}$ and $f_{\max} = f_0 + B/2 = 8.0\,\text{GHz}$. As can be noticed in Fig. 6(a), the antenna with the described geometry turns to be well-matched to the feeding waveguide in a pretty wide band around the resonant frequency $f_r \simeq 7.075\,\text{GHz}$ corresponding to the peak value of the return loss.

Using the *SEM*-based approach described in [3], a spherical harmonic representation of the equivalent surface current densities excited on the Huygens sphere S_h with radius $R_h = 5.5\,\text{cm}$ have been computed on-the-fly in step with the numerical $FDTD$ simulation, and then fitted to a pole/residue expansion with orders $N = 10$ and $K = 20$ selected heuristically in such a way as to ensure an adequate degree of accuracy in the modeling of the natural resonant processes occurring in the structure. The resulting resonant pole distribution in the complex frequency domain is shown in Fig. 6(b). The pair of conjugate dominant poles with minimal damping coefficient value $\sigma_p \simeq -0.68 \times 10^9\,\text{s}^{-1}$ can be readily noticed. The relevant mode is characterized by resonant frequency $f_p = \frac{1}{2}\omega_p/\pi \simeq 7.025\,\text{GHz}$, in good agreement with the return-loss response of the antenna (see Fig. 6(a)). In this way, the transient

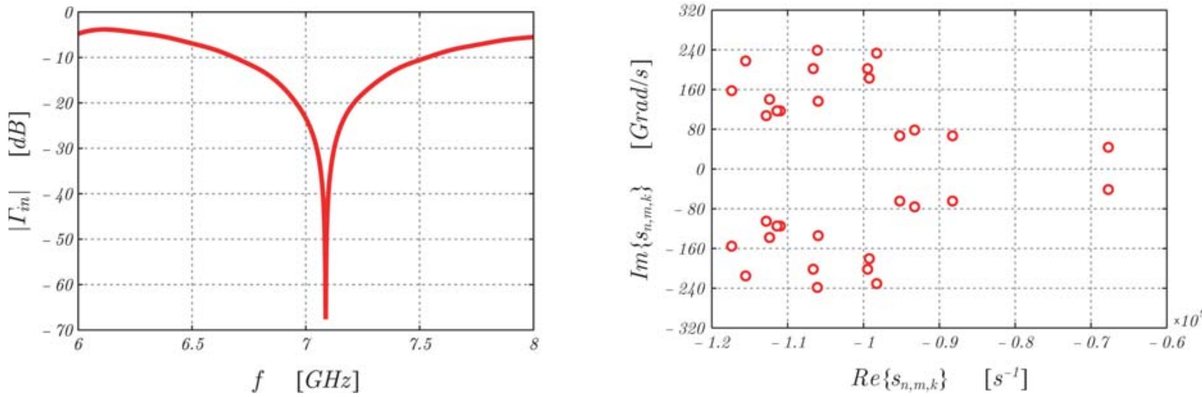

(a) (b)

Figure 6. Frequency-domain behavior of the input reflection coefficient (a) and distribution of the resonant poles, (b) featured by the hemispherical dielectric lens antenna shown in Fig. 1.

electromagnetic field radiated outside S_h can be evaluated, without any limitation involving the time, by using Equations (1) and (2) in combination with the analytical closed-form expression (14) of the general *IMSBF*. On the other hand, the electromagnetic field behavior in the frequency domain can be readily derived by application of the unilateral Laplace transform operator $\mathcal{L}_t\{\cdot\}$ to both sides of (1) and (2). So, making judicious use of the time scaling and frequency shifting properties of $\mathcal{L}_t\{\cdot\}$ yields, after some algebra, the following vector representation:

$$\begin{aligned} \boldsymbol{E}(\mathbf{r},p) &= \mathcal{L}_t\{\mathcal{E}(\mathbf{r},\tau)\}(p) = \int_0^{+\infty} \mathcal{E}(\mathbf{r},\tau)\, e^{-pt} dt \\ &= t_h \frac{e^{-jk_0 r}}{4\pi r c_0} \sum_{n=0}^{N} \sum_{m=-n}^{n} \sum_{k=1}^{K} \Psi_n(s_{n,m,k} t_h, p t_h)\, Y_n^m(\vartheta,\varphi)\, \mathbf{e}_{n,m,k}, \end{aligned} \tag{29}$$

$$\boldsymbol{H}(\mathbf{r},p) = \mathcal{L}_t\{\mathcal{H}(\mathbf{r},\tau)\}(p) = \frac{1}{\eta_0} \hat{\mathbf{r}} \times \boldsymbol{E}(\mathbf{r},p), \tag{30}$$

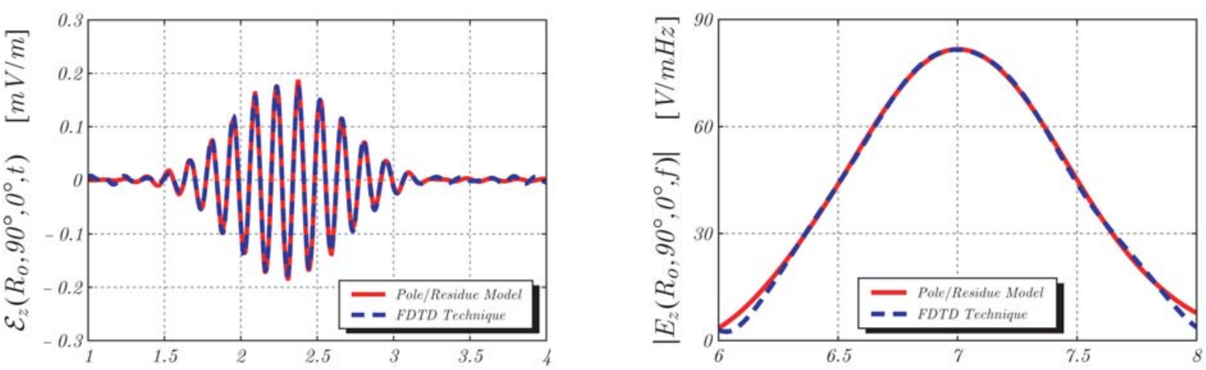

(a) (b)

Figure 7. Transient (a) and frequency-domain, (b) behavior of the co-polarized electric field component excited by the hemispherical dielectric lens antenna shown in Fig. 1 at a distance $R_O = 6.0\,\mathrm{cm}$ from the ground plane along the boresight direction (x-axis in the adopted coordinate system).

with $k_0 = -jp/c_0$ denoting the complex wavenumber in free space, and where [see Equation (31)]:

$$\Psi_n(\xi, p) = \mathcal{L}_w\{\psi_n(\xi, w)\}(p) = \int_0^{+\infty} \psi_n(\xi, w)\, e^{-pw} dt = \frac{i_n(p)}{p/\xi - 1}. \tag{31}$$

As in Fig. 7, the agreement with the numerical results obtained using the aforementioned full-wave locally conformal *FDTD* technique is pretty good. But, it is here worth stressing that the computational times and memory usage required to derive the pole/residue spherical harmonic expansion of the radiated electromagnetic field are just negligible in comparison with those relevant to the *FDTD*-based simulation aimed at computing the antenna far-field distribution. Furthermore, the fully numerical modeling approach is unable to provide an integral physical insight into the mechanisms which are responsible for the electromagnetic behavior of the structure under analysis. As far as the considered test case is concerned, it is apparent from Fig. 7 that the late-time characteristics of the radiating structure are primarily determined by the pair of dominant poles, whereas the poles having larger damping coefficients affect and shape mainly the very early transient response.

The extension of the presented theoretical formulation to the analytical time-domain modeling of general linear arrays [14] is currently ongoing and will be detailed in a separate research paper.

5. CONCLUSIONS

A new sequence of special polynomials for electromagnetics and mathematical physics has been presented. This class, formed by the incomplete Bessel polynomials, can be usefully employed to describe electromagnetic radiation and diffraction phenomena regarding truncated spherical structures. The general properties of the considered functions have been derived and discussed. In particular, the differential and recurrence equations feature additional terms with respect to those relevant to the classical Bessel polynomial theory.

By using said class of special functions, the transient electromagnetic field radiated by a general antenna can be determined in analytical closed form as the superposition of non-uniform spherical waves attenuating along with the radial distance and time according to the complex poles related to the resonant processes occurring in the structure. The presented formulation gives a meaningful insight into the physical mechanisms which are responsible for the electromagnetic behavior of a radiating structure, and can be used to optimize the performance of antennas for a wide variety of applications.

ACKNOWLEDGMENT

This research has been partly carried out in the framework of the research and development program at The Antenna Company Nederland B.V. and the project 8.909.2014/K funded by the Ministry of Education and Science of the Russian Federation.

REFERENCES

1. Andrews, G. E., R. Askey, and R. Roy, *Special Functions*, Cambridge Univ. Press, 2001.
2. Cicchetti, R. and A. Faraone, "Incomplete Hankel and modified Bessel functions: A class of special functions for electromagnetics," *IEEE Trans. Antennas Propag.*, Vol. 52, No. 12, 3373–3389, 2004.
3. Caratelli, D. and A. Yarovoy, "Unified time- and frequency-domain approach for accurate modeling of electromagnetic radiation processes in ultra-wideband antennas," *IEEE Trans. Antennas Propagat.*, Vol. 58, No. 10, 3239–3255, 2010.
4. Caratelli, D. and A. Yarovoy, "Incomplete modified spherical Bessel functions: a new class of special functions for electromagnetics," *Proc. 20th International Symposium on Electromagnetic Theory*, 289–292, Berlin, Germany, 2010.
5. MacRobert, T. M. and I. N. Sneddon, *Spherical Harmonics: An Elementary Treatise on Harmonic Functions with Applications*, Pergamon Press, 1967.
6. Abramowitz, M. and I. A. Stegun, *Handbook of Mathematical Functions*, Dover, 1962.
7. Watson, G. N., *A Treatise on the Theory of Bessel Functions*, Cambridge Univ. Press, 1962.

8. Luke, Y., *The Special Functions and Their Approximations*, Academic Press, 1969.
9. Krall, H. L. and O. Frink, "A new class of orthogonal polynomials: The Bessel polynomials," *Trans. Amer. Math. Soc.*, Vol. 65, No. 1, 100–115, 1948.
10. Grosswald, E., *Bessel Polynomials (Lecture Notes in Mathematics)*, Springer-Verlag, 1978.
11. Thomson, W. E., "Delay networks having maximally flat frequency characteristics," *Proc. IEE*, Vol. 96, Part III, 487–490, 1949.
12. Caratelli, D., A. Massaro, R. Cingolani, and A. Yarovoy, "Accurate time-domain modeling of reconfigurable antenna sensors for non-invasive melanoma skin cancer detection," *IEEE Sensors J.*, Vol. 12, No. 3, 635–643, 2012.
13. Taflove, A. and S. C. Hagness, *Computational Electrodynamics: The Finite Difference Time Domain Method*, Artech House, 2005.
14. Caratelli, D. and M. C. Viganó, "Analytical synthesis technique for linear uniform-amplitude sparse arrays," *Radio Sci.*, 2011, 10.1029/2010RS004522.